ELSEVIER

Contents lists available at ScienceDirect

# Analytica Chimica Acta

journal homepage: www.elsevier.com/locate/aca



# Infrared laser ablation and capture of enzymes with conserved activity



Kelin Wang, Fabrizio Donnarumma, Matthew D. Baldone, Kermit K. Murray\*

Department of Chemistry, Louisiana State University, Baton Rouge, Louisiana, 70803, United States

#### HIGHLIGHTS

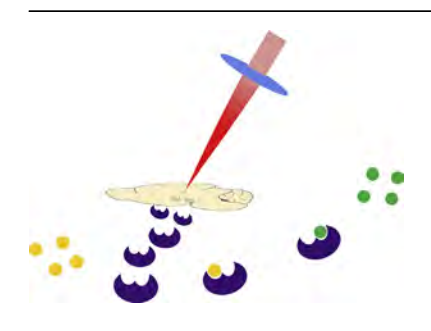
- Laser ablation and capture of enzymes from rat brain.
- Enzymes transferred with 75% efficiency with laser fluences in 10
   -30 kJ/m² range.
- 37% of the transferred trypsin was active while 50% of transferred catalase was active.
- Catalase activity measured from ablation transferred rat brain tissue tracks anticipated catalase activity distribution.

## ARTICLE INFO

Article history: Received 19 January 2018 Received in revised form 16 April 2018 Accepted 22 April 2018 Available online 26 April 2018

Keywords: Enzyme activity MALDI Laser ablation Fluorescence assay Trypsin Catalase

#### G R A P H I C A L A B S T R A C T



## ABSTRACT

Infrared (IR) laser ablation at 3  $\mu m$  wavelength was used to extract enzymes from tissue and quantitatively determine their activity. Experiments were conducted with trypsin, which was ablated, captured and then used to digest bovine serum albumin (BSA). BSA digests were evaluated using matrix-assisted laser desorption ionization (MALDI) mass spectrometry (MS) and sequence coverage of 59% was achieved. Quantification was performed using trypsin and catalase standards and rat brain tissue by fluorescence spectroscopy. Both enzymes were reproducibly transferred with an efficiency of 75  $\pm$  8% at laser fluences between 10 and 30 kJ/m². Trypsin retained 37  $\pm$  2% of its activity and catalase retained 50  $\pm$  7%. The activity of catalase from tissue was tested using three consecutive 50  $\mu$ m thick rat brain sections. Two 4 mm² regions were ablated and captured from the cortex and cerebellum regions. The absolute catalase concentration in the two regions was consistent with previously published data, demonstrating transfer of intact enzymes from tissue.

© 2018 Elsevier B.V. All rights reserved.

#### 1. Introduction

Enzyme histochemistry combines the measurement of enzyme activity with localization information and serves as a link between biochemistry and morphology [1]. Enzyme histochemistry has been used in diagnostic pathology and pathobiology, as well as in experimental pathology [2]. The activity of an enzyme is regulated

E-mail address: kkmurray@lsu.edu (K.K. Murray).

at different levels from mRNA to post translational modifications [3, 4] and from molecular interactions between the cytoplasm and organelles to other regulation mechanisms in the extracellular matrix [5]. Accordingly, the full picture of enzyme activity cannot be determined simply by total protein or mRNA quantification.

Imaging of fresh frozen tissue sections and biopsies using methods such as fluorescent probes, chromogenic probes, and *in situ* zymography [6, 7] allows measurement of enzyme activity with localization information. In the case of fluorescent or chromogenic agents, probes can be sprayed on the tissue section before measuring the localized signal [8, 9]. After enzyme reaction on the surface of the tissue section, the localized indicator is activated

<sup>\*</sup> Corresponding author. 331 Choppin Hall, Department of Chemistry, Louisiana State University, Louisiana, 70803, United States.

based on enzyme activity [8-10]. Similarly, *in situ* zymography is an electrophoretic technique that uses fluorescent or chromogenic reactions [11]. There are two general zymography methods [6, 12]: tissue sections can be mounted on a glass slide coated with a fluorescent substrate, or first mounted on a slide, then immersed in a solution containing fluorescent substrate. Unlike fluorescent or chromogenic probes that are able to detect various enzymes [8, 9, 13, 14], the substrates used for zymography are typically protein based [15, 16], such as gelatin or collagen, which make *in situ* zymography well suited for proteases [17]. Imaging based methods require special probes, the design of which can be challenging due to time consuming steps, high costs, [18] and their potential for non-specific binding [19].

Extraction of enzymes from small regions of tissue sections allows the measurement of localized enzyme activity [20, 21]. Regions of interest (ROI) containing enzymes can be isolated via manual microdissection followed by extraction and analysis. Extraction from microdissected tissue allows measurement of isolated cell populations in solution rather than on the tissue section surface. This enables more flexibility in adjustment of reaction conditions such as temperature and pH, which can play an important role on reproducibly of enzyme assay [22]. In addition, extraction of enzymes can facilitate absolute quantification of their activity, whereas imaging techniques are often limited to relative quantification [23-25]. Although ROI can be isolated by manual microdissection, where the material is removed under an optical microscope [21, 26], this technique is somewhat labor intensive and has limited reproducibility [27].

An alternative dissection technique is laser capture microdissection (LCM) [28], which employs a focused laser to cut and isolate regions from a tissue section. There are two general LCM configurations that use either an infrared (IR) or ultraviolet (UV) laser [28, 29]. IR-LCM employs a thin thermoplastic film that covers a tissue section. A near IR laser is used to irradiate and melt part of the film, causing it to fuse with that part of the tissue section. The film is detached together with the tissue material [30]. UV-LCM uses a UV laser to cut the boundary of a ROI on a tissue section and the ROI is then detached using unfocused laser pulses [31]. In both LCM configurations, collected tissue regions require extraction and cell lysis before measuring enzyme activity [20].

An alternative to LCM is laser ablation and capture, where the region of interest is removed with a pulsed infrared laser [32, 33]. The ejected material is collected and biomolecules can be extracted without the need of cell lysis or addition of detergents [32-34]. The main absorber of infrared laser radiation in tissue is water, which as an absorption maximum at 2.94  $\mu m$  [35]. The optical penetration depth is approximately 1 µm at room temperature, but increases with temperature, facilitating greater material removal at higher pulse energies [36]. Another tissue absorber is protein, which has OH and NH stretch absorbers at 3 µm and CH stretch absorbers at 3.4 µm. Absorption at these wavelengths can produce ablation of proteins even in nominally dry samples [37]. Absorption of pulsed nanosecond mid-IR laser light is sufficiently rapid to produce a volumetric phase change and explosive boiling of the irradiated volume [38, 39]. The recoil stress of the phase explosion leads to the ejection of particulate with size distributions that vary with laser energy and the mechanical strength of the tissue [38, 40]. The removal of material as particulate appears to protect fragile biomolecules from fragmentation allowing the capture of intact peptides, proteins [33], and DNA [34] from tissue using a nanosecond laser. Near-IR and mid-IR picosecond lasers can even more efficiently produce explosive boiling in tissue and have been employed to ablate and capture cells, virus and proteins with conserved function and activity [41-43].

In the work described below, enzymes from thin films as well as

from tissue sections were ablated and captured using a nanosecond mid-IR laser, and their activity quantitatively assessed. Trypsin and catalase enzyme standards were laser ablated using a 3  $\mu m$  wavelength laser and the transfer efficiency was measured using Bradford assay while the activity of trypsin was qualitatively assessed by using it to digest bovine serum albumin (BSA) before analysis by MALDI mass spectrometry. Quantitative assessment of the activity of trypsin and catalase standards after laser ablation was measured using fluorescence assays and the activity of catalase ablated and captured from rat brain tissue sections was determined.

## 2. Experimental

# 2.1. Chemicals and materials

Sequencing grade modified trypsin was purchased from Promega (Madison, WI, USA). Reagents DL-dithiothreitol (DDT, 98%), iodoacetamide (IAA, BioUltra, 99%),  $\alpha$ -cyano-4-hydroxycinnamic acid (CHCA), and ammonium bicarbonate (ABC, BioUltra, 99.5%) were obtained from Sigma-Aldrich (St Louis, MO, USA). Trifluoroacetic acid (99.5%, LC-MS grade) and acetonitrile (99.9%, LC-MS grade) were obtained from Thermo Fisher Scientific (Waltham, MA, USA). Bovine serum albumin (BSA) and glass microscope slides  $(25\times75\,\mathrm{mm})$  were obtained from VWR (Radnor, PA). BSA from VWR was used as substrate for trypsin digestion. Ultrapure water (18  $\mathrm{M}\Omega$ ) was produced with a Barnstead Nanopure Diamond Lab Water System (Thermo Fisher Scientific). The ABC buffer was prepared at a concentration of 10 mM and corrected to a pH of 7.4.

A Bradford assay kit (Coomassie Plus, Thermo Fisher Scientific), which included Coomassie dye and BSA protein standard, was used to build calibration curves for protein quantification. A fluorescent protease assay kit (Pierce, Thermo Fisher Scientific) included L-(tosylamido-2-pheyl) ethyl chloromethyl ketone (TPCK) treated trypsin, fluorescein isothiocynante (FTIC) labelled casein, and tris buffered saline (TBS; 25 mM tris; pH 7.2, 150 mM NaCl). An Amplex Red catalase assay kit (Life Technologies, Grand Island, NY, USA) included Amplex Red reagent, dimethylsulfoxide (DMSO), horseradish peroxidase, hydrogen peroxide, reaction buffer, and catalase.

#### 2.2. Sample preparation

Enzymes were reconstituted in TBS or fluorescence reaction buffers and BSA was dissolved in 10 mM ABC buffer (pH 7.4) at a concentration of 0.5 mg/mL. Aliquots of the enzyme solutions were deposited on a plain microscope slide (cleaned with ethanol) and dried for 2 min under vacuum before ablation.

Sprague Dawley rat brain tissue samples were collected from 6 week old rats using procedures approved by the LSU Institutional Animal Care and Use Committee (IACUC) at the LSU School of Veterinary Medicine, Division of Laboratory Animal Medicine (DLAM). The animals were sacrificed by carbon dioxide exposure and tissue samples were collected and snap-frozen within 30 min using liquid nitrogen and stored at  $-80\,^{\circ}\text{C}$  prior to use. Frozen tissue was sectioned at a thickness of 50  $\mu\text{m}$  and thaw-mounted on the microscope slide at  $-20\,^{\circ}\text{C}$  using a cryostat (CM 1850, Leica Microsystems, Wetzlar, Germany). Optimal cutting temperature solution (OCT, Sakura Finetek, USA) was used to fix one side of the brain tissue sample to the cryostat support. Slides were stored at  $-80\,^{\circ}\text{C}$  until further processing and were vacuum dried for 10 min prior to sampling.

# 2.3. Laser ablation sample transfer

The mid-IR laser ablation system has been described in detail previously [33, 44]. Briefly, a wavelength tunable pulsed IR optical

parametric oscillator (IR Opolette, OPOTEK, Carlsbad, CA, USA) was used to ablate samples mounted on microscope slides. The wavelength was 2.94 µm to overlap with OH stretch absorption [37] and the repetition rate was 20 Hz. The pulse temporal width of the OPO is 7 ns and the beam diameter is 4 mm. The laser was directed at the sample target at normal incidence and focused with a 50 mm focal length lens to a spot size of 200 × 300 um determined by burn paper at 2 mI laser energy. The spot size of a single shot on a 50 um rat brain tissue section at 1.1 mJ pulse energy was  $100 \times 140 \,\mu m$ . The laser was attenuated internally using laser control software to fluences between 10 and 30 kJ/m<sup>2</sup>. The microscope slides were mounted on two orthogonal linear stages (Model 443, Newport, Irvine, CA, USA) that were translated with 50 mm motorized actuators (LTA-HS, Newport) using a motion controller (XPS-Q8, Newport). A microcentrifuge tube with TBS buffer or reaction buffer was mounted 5 mm below the microscope slide to collect the ablated material. The actuators were operated at a velocity of 1 mm/s using a serpentine pattern with 100 µm raster line spacing. A schematic of the laser ablation and capture system is shown in Fig. S1 of the supplementary material.

# 2.4. BSA digestion

Four aliquots of 50  $\mu$ l BSA (from VWR) at a concentration of 0.4 mg/mL were used as the substrate for trypsin digestion. Disulfide bond reduction was achieved by adding DTT to each tube to a final concentration of 10 mM, and samples were incubated at 80 °C for 45 min. Alkylation was performed by adding IAA to a final concentration of 20 mM with incubation in the dark for 30 min. Laser ablated and captured trypsin was vacuum dried and resuspended in 2  $\mu$ l of ABC buffer, and compared to control samples of trypsin without laser ablation. Samples were incubated in a 37 °C shaker at 600 rpm overnight.

# 2.5. Mass spectrometry

Mass spectra were acquired using a MALDI-TOF/TOF mass spectrometer (UltrafleXtreme; Bruker Daltonics, Billerica, MA, USA) operated in reflectron mode. Each spectrum was produced by summing 500 individual spectra obtained at 1000 Hz repetition rate in partial sample random walk mode. Raw data were processed with FlexAnalysis 3.3 (Bruker). A tryptic peptide peak list was generated with maximum two missed cleavages, cysteine carbamidomethylation, and methionine oxidation. A mass tolerance of 250 ppm was used.

# 2.6. Protein concentration estimation

Enzyme and protein concentrations were measured with a Bradford colorimetric assay [45]. Calibration curves for enzyme concentration were obtained in triplicate using control aliquots of the target enzyme (SI Fig.S3 and Fig. S4). Calibration curves for the ablated proteins were obtained in triplicate using BSA standards from Bradford colorimetric assay.

#### 2.7. Enzyme activity analysis

Trypsin activity was measured using the fluorescent protease assay kit according to the manufacturer's protocol. Briefly, trypsin at a range of concentrations up to 5 mg/L was mixed with 100  $\mu L$  of fluorescein isothiocyanate (FTIC) labelled casein (100 mg/L in TBS) and incubated at room temperature. Fluorescence was measured after 60 min incubation using a microplate reader at excitation and emission wavelengths of 435 and 538 nm, respectively, and expressed as relative fluorescence units (RFU; SI Fig. S5 and S6).

Catalase activity analysis was performed using the Amplex Red assay kit following the manufacturer's protocol. Briefly, calibration curves were generated using catalase at concentrations ranging from 0 to 1 U/mL, where 1 unit is defined as the amount of enzyme that will decompose 1.0  $\mu$ mole of  $H_2O_2$  per minute at pH 7.0 at  $25\,^{\circ}$ C. Samples and calibrants were incubated with  $40\,\mu$ M  $H_2O_2$  for  $30\,m$ in at room temperature in the dark and then mixed with  $100\,\mu$ M Amplex Red reagent at  $37\,^{\circ}$ C. Fluorescence emission was measured after incubation for  $30\,m$ in and  $45\,m$ in using a microplate reader (Wallac 1420 Victor 2; PerkinElmer, Waltham, MA, USA). Excitation and emission wavelengths of 571 nm and 585 nm were used (SI Fig. S5). Background fluorescence was obtained from buffer-containing sample wells and subtracted from all data points.

#### 3. Results and discussion

Initial experiments were directed at qualitatively assessing the presence of enzymatic activity after IR laser ablation. These experiments were aimed at assessing the effect of laser sampling on enzymes in absence of the tissue matrix. Trypsin (2  $\mu$ L, ~1000 ng) was deposited on a microscope slide, vacuum-dried, and the thin film was completely ablated at a laser fluence of 18 kJ/m² and collected in a 200  $\mu$ l volume of ABC buffer. Aliquots of BSA were either digested with the ablated and captured trypsin or with a control solution containing the same amount of enzyme deposited on the slide before ablation. BSA digests were analyzed by MALDI mass spectrometry. Figure 1 shows representative mass spectra of BSA tryptic peptides obtained using ablation capture and control trypsin. The peaks corresponding to protonated tryptic peptides with the intensity >1000 are indicated with circles. The laser ablated trypsin yielded a similar spectrum compared to the control

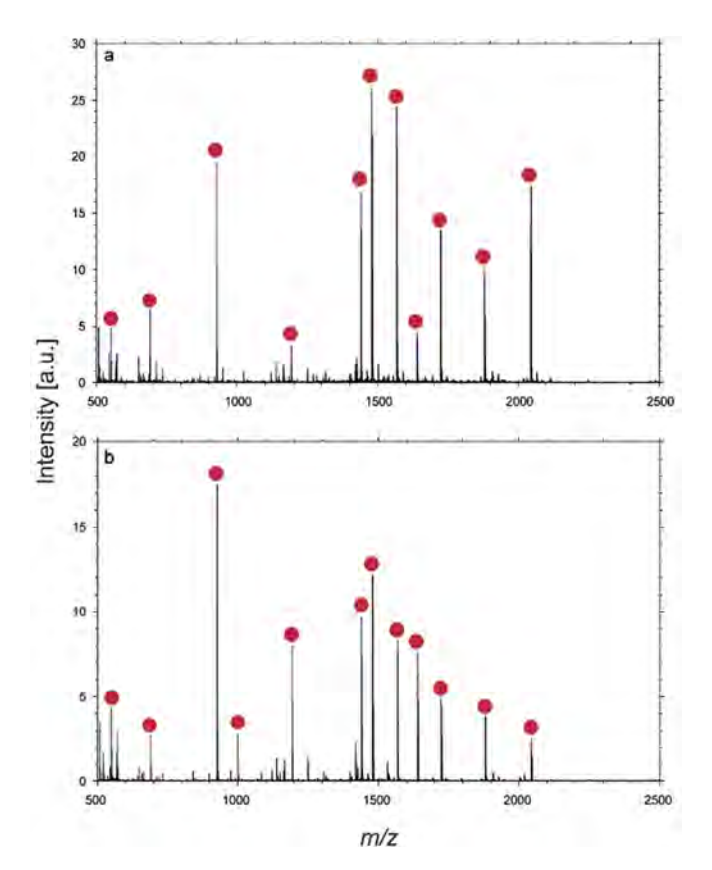


**Figure 1.** MALDI mass spectra of BSA tryptic peptides (circles) obtained from (a) trypsin control and (b) laser ablation transferred trypsin.

with respect to the number and m/z of the peaks, although the intensity was about half as large. Table S1 reports the sequences of all identified tryptic peptides together with their measured m/z, theoretical m/z and mass error. Figure S2 shows the sequence coverage. A total of 42 tryptic peptides, corresponding to 61% sequence coverage, were identified for the control, whereas 44 peptides, corresponding to 59% sequence coverage, were identified with the ablated trypsin. The signal intensity and lower sequence coverage may result from either low efficiency of trypsin ablation and capture or from loss of enzyme activity of the ablated and captured trypsin.

The ablation and capture transfer efficiency can be defined as the ratio of the captured enzyme (both active and inactive) to the quantity of material ablated. To determine the capture efficiency, thin films of trypsin and catalase were ablated at various laser energies and the total protein was determined by Bradford assay. Dried sample deposits containing 4 µg of trypsin were ablated at laser fluences of 10, 18, and 26 kJ/m<sup>2</sup> and the enzyme was captured in TBS buffer. A Bradford assay was used to measure the trypsin concentration from 3 replicate samples at each laser energy and from control samples. Figure 2a shows the transfer efficiency of trypsin (dark grey) and catalase (light grey). The resulting transfer efficiency was approximately  $73 \pm 9\%$  at all fluences:  $74 \pm 8\%$  at  $10 \text{ kJ/m}^2$ ,  $71 \pm 6\%$  at  $18 \text{ kJ/m}^2$ , and  $74 \pm 13\%$  at  $26 \text{ kJ/m}^2$ . The transfer efficiency for catalase was measured in a similar manner. Sample deposits containing 0.5 unit catalase were ablated and captured in buffer, and analyzed by Bradford assay. The measured transfer efficiency was similar to that recorded for trypsin:  $73 \pm 7\%$  at 10 kJ/ $m^2$ , 79 ± 5% at 18 kJ/ $m^2$ , and 75 ± 7% at 26 kJ/ $m^2$ .

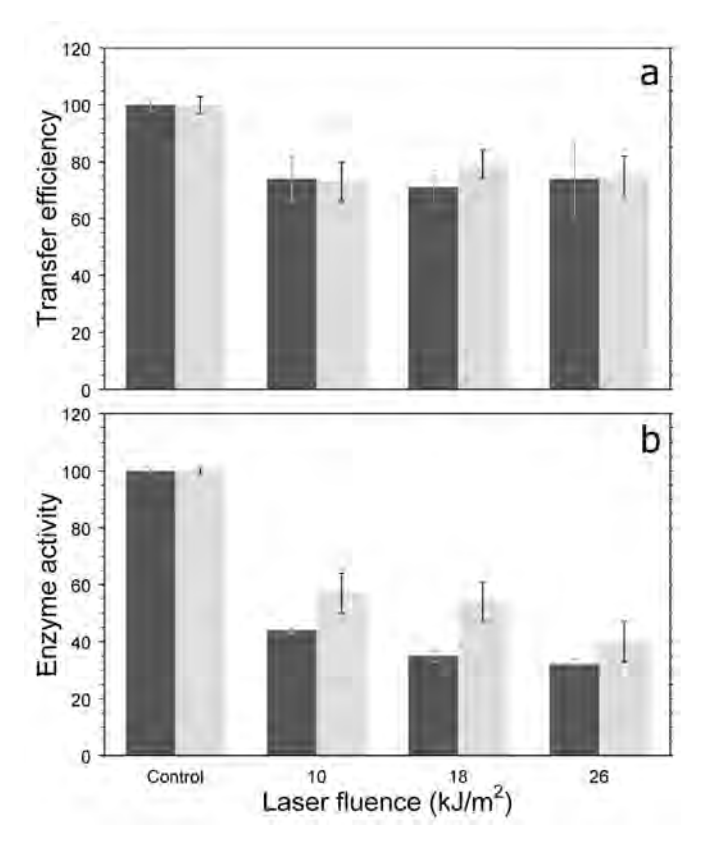


**Figure 2.** Transfer efficiency and activity of enzyme ablated at laser fluences of 10, 18,  $26 \, k \rfloor m^2$ : (a) enzyme transfer efficiency was measured using Bradford assay; (b) enzyme activity obtained using a catalase fluorescence assay; control for trypsin (dark grey) is  $4 \, \mu g$ , for catalase (light grey) is 0.5 U. All experiments were conducted in triplicate.

Experiments were performed to determine the activity of the laser ablation transferred enzymes using a protease fluorescence assay. Sample deposits containing 4 µg trypsin were ablated and captured at laser fluences of 10, 18, and 26 kJ/m<sup>2</sup> and captured in TBS buffer. Figure 2b shows the trypsin activity (dark grey) obtained with the fluorescence assay:  $44 \pm 1\%$  at  $10 \text{ kJ/m}^2$ ,  $35 \pm 2\%$  at  $18 \text{ kJ/m}^2$ , and  $32 \pm 2\%$  at  $26 \text{ kJ/m}^2$  compared to the activity of the control. To determine the activity of the laser ablation captured catalase, samples containing 0.5 U catalase were ablated and captured in the assay kit buffer solution. Figure 2b shows the activity of the catalase (light grey) determined by fluorescence assay:  $57 \pm 7\%$  at  $10 \text{ kJ/m}^2$ ,  $54 \pm 7\%$  at  $18 \text{ kJ/m}^2$ , and  $40 \pm 7\%$  at  $26 \text{ kJ/m}^2$ . These results indicate that approximately  $37 \pm 2\%$  of the transferred trypsin is active and approximately  $50 \pm 7\%$  of the transferred catalase is active and the activity is approximately one third lower at the highest laser energy. The loss of activity may result from heating and denaturation of the enzyme during laser ablation. Although infrared laser ablation has previously been shown to transfer proteins and DNA intact [32, 34], the heating may be great enough to denature a fraction of the enzyme molecules.

The trypsin activity results described in Figure 1 are consistent with previous studies using picosecond mid-infrared laser ablation of protein with conserved activity [46, 47]. This study also demonstrated that enzymes in human plasma ablated with a picosecond laser are still active. The 70% transfer efficiency of protein material reported here is similar to that previously observed for mid-IR picosecond laser ablation capture of intact bacterial cells that subsequently were used to grow bacterial colonies [42].

The effect of laser ablation on the activity of enzymes captured from tissue was studied using thin tissue sections. Here, the IR laser system was used to ablate material from sections of rat brain tissue mounted on microscope slides. Rat brain tissue sections 50 µm thick were used. This allowed retrieval of more material per unit area compared to thinner samples. It was found that a fluence of 10 kJ/m<sup>2</sup> was not sufficient to completely ablate the tissue, therefore a fluence of 18 kJ/m<sup>2</sup> was used for these studies. Two spots of 4 mm<sup>2</sup> area from each tissue section (three tissue sections in total) were ablated and captured in  $100 \, \mu l$  of reaction buffer. The captured material was divided into a 50 µl aliquot for total protein analysis by Bradford assay and a 25 µl aliquot for catalase activity determination. Figure 3a shows a bright-field microscope image of a sagittal tissue section with the ablated areas, corresponding to the frontal cortex (Section 1) and the cerebellum (Section 2). The samples obtained from the cerebellum and frontal cortex yielded  $2.7 \pm 0.1 \,\mu g$  and  $2.5 \pm 0.1 \,\mu g$  total protein, respectively. According to manufacturer's protocol, the catalase activity of the ablated and collected tissue was measured after 30 and 45 min. At 30 min, the catalase activity obtained from the cerebellum region was  $11.2 \pm 0.7$ mU/mm<sup>2</sup> from the frontal cortex  $8.0 \pm 0.7$  mU/mm<sup>2</sup>. At 45 min, the activity was  $10.7 \pm 0.7 \text{ mU/mm}^2$  from the cerebellum and  $7.5 \pm 0.7$ mU mm<sup>2</sup> from the frontal cortex. The catalase activity was normalized to the total protein in the captured sample to allow quantitative comparison of the activity in the different brain regions. The cerebellum catalase activity was  $16.3 \pm 0.3$  and  $16.0 \pm 0.2$ U/mg for 30 and 45 min, respectively, whereas the frontal cortex activity was  $12.5 \pm 0.3$  and  $12.0 \pm 0.3$  U/mg.

Taking into consideration the inhomogeneous water content of tissue samples [48] and the mechanical strength of the tissue matrix [38], tissue samples may not be ablated as efficiently as pure enzymes. Nonetheless, the quantity of catalase captured from tissue is generally consistent with previously reported results, suggesting that the efficiency of transfer of active enzyme from tissue is comparable to that from dried-droplet samples. However, it must be noted that measuring catalase activity in tissue poses several

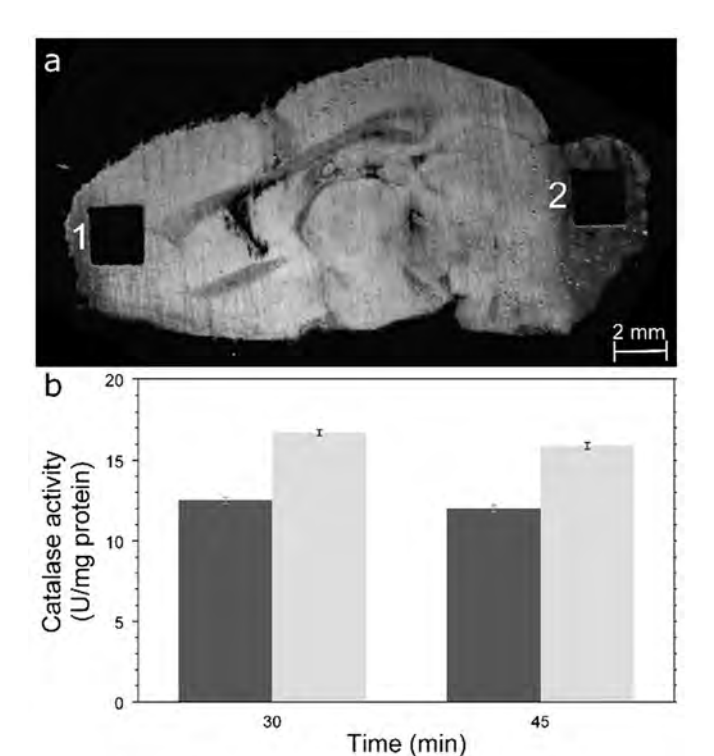


**Figure 3.** (a) Bright-field microscope image of laser ablation sampled rat brain tissue (1) frontal cortex and (2) cerebellum and (b) catalase activity from a fluorescence assay frontal cortex (grey) and cerebellum (light grey) at 30 and 45 min.

challenges. For example, the absolute activity in several brain compartments can vary as a function of rat age [49]. For this reason, the variation in catalase activity reported in various studies can be significant. The catalase activity in male albino Wistar rats was reported by Homi et al. to be 1.9 U/mg in the cortex and 3 U/mg in the cerebellum [50] and Jayaraman et al. reported values of 3 U/mg in the cortex and 4 U/mg in the cerebellum [51]. Sigueira et al reported catalase activity equal to 0.4 U/mg in the cortex and 0.8 U/ mg in the cerebellum of male Wistar rats [49]. Kazi et al. reported 1 U/mg in the cortex and 1.5 U/mg in the cerebellum of female Wistar rats [52]. Compared to the data above, Fortunato et al. reported lower absolute values of catalase in Wistar rat cortex and cerebellum. Using 6 animal in each control group, they reported values for the cortex differing over 5 times from each other, with numbers ranging from 0.0002 to 0.001 U/mg. In the cerebellum, they reported values differing over 20 times from each other, with values ranging from 0.0002 to 0.0035 U/mg [53]. In the IR laser ablation study a different breed of rat was used, which may explain the higher catalase activity measured. In addition, catalase activity was measured using laser ablated extract from consecutive sections the same rat brain whereas the published literature reports activity from multiple animals. At the same time, the catalase activity obtained from ablated and captured sample replicates was measured with relative standard deviation ranging from 1 to 2.5% which demonstrates the high reproducibility of the method.

## 4. Conclusions

The results above demonstrate that enzymes can be IR laser ablated and captured from solid samples and from tissue while maintaining activity. The transfer efficiency of total protein was approximately  $75\pm8\%$  with about  $2.5\,\mu g$  protein obtained from  $4\,mm^2$  of rat brain tissue, results which are consistent with

previous studies of laser ablation transfer of proteins [32]. Approximately one-third of the captured trypsin and one-half of the captured catalase retained enzyme activity as determined by fluorescence assay. The enzyme catalase was ablated and captured from rat brain tissue and the absolute activity measured was consistent with that anticipated for the different regions of the brain, suggesting that active enzymes can be efficiently ablated and captured from tissue. Due to the fast sampling speed, measurement of laser ablated and captured endoproteases and oxidoreductases can be used as a complementary tool to pathohistological evaluation of tissue in application such as surgery and tissue classification.

Future work will combine enzyme assays with liquid chromatography and mass spectrometry for protein identification [32] and with polymerase chain reaction for DNA analysis [34] of laser ablated and captured tissue. While the current speed of both laser and translation allows for fast sampling for offline analyses of mm<sup>2</sup> sized ROIs, compatibility of laser ablation with mass spectrometry imaging will require a higher repetition rate laser as well as a smaller spot size to improve the lateral resolution.

#### Compliance with ethical standards

Conflict of interest

The authors declare that they have no conflict of interest.

## Acknowlegements

This material is based upon work supported by the National Science Foundation under Grant No. DBI-1556000 and CHE-1709526 The authors thank Dr. D. G. Baker (School of Veterinary Medicine, Louisiana State University) for kindly providing rat brain samples and the Louisiana State University Mass Spectrometry Facility for the MALDI analysis.

## Appendix A. Supplementary data

Supplementary data related to this article can be found at https://doi.org/10.1016/j.aca.2018.04.058.

## References

- [1] J. Estabel, Enzyme histochemistry methods, in: J.M. Exbrayat (Ed.), Histochemical and Cytochemical Methods of Visualization, CRC Press, Boca Raton, 2013, pp. 139–146.
- [2] W.A. Meier-Ruge, E. Bruder, Current concepts of enzyme histochemistry in modern pathology, Pathobiology 75 (2008) 233—243.
- [3] M. Bogyo, B.F. Cravatt, Genomics and proteomics: from genes to function: advances in applications of chemical and systems biology, Curr. Opin. Chem. Biol. 11 (2007) 1—3.
- [4] C.J. Van Noorden, Metabolic mapping by enzyme histochemistry in living animals, tissues and cells, J Physiol. Pharmacol. 60 (2009) 125–129.
- [5] C.J. Van Noorden, Imaging enzymes at work: metabolic mapping by enzyme histochemistry, J. Histochem. Cytochem. 58 (2010) 481–497.
- [6] J. Vandooren, N. Geurts, E. Martens, P.E. Van den Steen, G. Opdenakker, Zymography methods for visualizing hydrolytic enzymes, Nat. Methods 10 (2013) 211–220.
- [7] W.M. Frederiks, O.R. Mook, Metabolic mapping of proteinase activity with emphasis on in situ zymography of gelatinases: review and protocols, J. Histochem. Cytochem. 52 (2004) 711–722.
- [8] N.P. Withana, M. Garland, M. Verdoes, L.O. Ofori, E. Segal, M. Bogyo, Labeling of active proteases in fresh-frozen tissues by topical application of quenched activity-based probes, Nat. Protoc. 11 (2016) 184–191.
- [9] G. Pampalakis, E. Zingkou, K. Vekrellis, G. Sotiropoulou, "Activography": a novel, versatile and easily adaptable method for monitoring enzymatic activities in situ, Chem. Commun. (Camb.) 53 (2017) 3246–3248.
- [10] A.K. Langton, C.E. Griffiths, M.J. Sherratt, R.E. Watson, Cross-linking of structural proteins in ageing skin: an in situ assay for the detection of amine oxidase activity, Biogerontology 14 (2013) 89–97.
- [11] J. van Smeden, I.M. Dijkhoff, R.W. Helder, H. Al-Khakany, D.E. Boer, A. Schreuder, W.W. Kallemeijn, S. Absalah, H.S. Overkleeft, J.M. Aerts, In-situ visualization of glucocerebrosidase in human skin tissue: zymography vs

- activity-based probe labeling, J. Lipid Res. 58 (2017) 2299-2309.
- [12] J. Wilkesman, L. Kurz, Zymography principles, in: J. Wilkesman, L. Kurz (Eds.), Zymography - Methods and Protocols, Springer, New York, 2017, pp. 3–10.
- [13] P. Yang, K. Liu, Activity-based protein profiling: recent advances in probe development and applications, Chem. Biochem. 16 (2015) 712–724.
- [14] J.M. Krysiak, J. Kreuzer, P. Macheroux, A. Hermetter, S.A. Sieber, R. Breinbauer, Activity-based probes for studying the activity of flavin-dependent oxidases and for the protein target profiling of monoamine oxidase inhibitors, Angew. Chem. Int. Ed. 51 (2012) 7035–7040.
- [15] S. Yan, E. Blomme, In situ zymography: a molecular pathology technique to localize endogenous protease activity in tissue sections, Vet. Pathol. 40 (2003) 227–236
- [16] J. Wilkesman, L. Kurz, Protease analysis by zymography: a review on techniques and patents, Recent Pat. Biotechnol. 3 (2009) 175–184.
- [17] P.M.C. Scaffa, L. Breschi, A. Mazzoni, C.d.M.P. Vidal, R. Curci, F. Apolonio, P. Gobbi, D. Pashley, L. Tjäderhane, I.L. dos Santos Tersariol, Co-distribution of cysteine cathepsins and matrix metalloproteases in human dentin, Arch. Oral Biol. 74 (2017) 101–107.
- [18] C.R. Ispas, G. Crivat, S. Andreescu, Recent developments in enzyme-based biosensors for biomedical analysis. Anal. Lett. 45 (2012) 168–186.
- [19] L.E. Sanman, M. Bogyo, Activity-based profiling of proteases, Annu. Rev. Biochem. 83 (2014) 249–273.
- [20] E. Abbott, D. Hall, B. Hamberger, J. Bohlmann, Laser microdissection of conifer stem tissues: isolation and analysis of high quality RNA, terpene synthase enzyme activity and terpenoid metabolites from resin ducts and cambial zone tissue of white spruce (Picea glauca), BMC Plant Biol. 10 (2010) 106.
- [21] J.W. Lee, C.-L. Chou, M.A. Knepper, Deep sequencing in microdissected renal tubules identifies nephron segment—specific transcriptomes, J. Am. Soc. Nephrol. 26 (2015) 2669–2677.
- [22] H. Bisswanger, Enzyme assays, Perspect. Sci. 1 (2014) 41–55.
- [23] R. Weissleder, M.J. Pittet, Imaging in the era of molecular oncology, Nature 452 (2008) 580.
- [24] G.D. Luker, K.E. Luker, Optical imaging: current applications and future directions, J. Nucl. Med. 49 (2008) 1–4.
- [25] D.P. Bishop, N. Cole, T. Zhang, P.A. Doble, D.J. Hare, A guide to integrating immunohistochemistry and chemical imaging, Chem. Soc. Rev. (2018), https://doi.org/10.1039/C7CS00610A.
- [26] P. Scherzer, A. Gal-Moscovici, D. Sheikh-Hamad, M.M. Popovtzer, Sodium-pump gene-expression, protein abundance and enzyme activity in isolated nephron segments of the aging rat kidney, Physiol. Rep. 3 (2015), e12369.
- [27] I.A. Eltoum, G.P. Siegal, A.R. Frost, Microdissection of histologic sections: past, present, and future, Adv. Anat. Pathol. 9 (2002) 316–322.
- [28] S. Datta, L. Malhotra, R. Dickerson, S. Chaffee, C.K. Sen, S. Roy, Laser capture microdissection: big data from small samples, Histol. Histopathol. 30 (2015) 1255—1269.
- [29] E. Jensen, Laser-capture microdissection, Anat. Rec. 296 (2013) 1683–1687.
- [30] M.R. Emmert-Buck, R.F. Bonner, P.D. Smith, R.F. Chuaqui, Z. Zhuang, S.R. Goldstein, R.A. Weiss, L.A. Liotta, Laser capture microdissection, Science 274 (1996) 998–1001.
- [31] K. Schüitze, G. Lahr, Identification of expressed genes by laser-mediated manipulation of single cells, Nat. Biotechnol. 16 (1998) 737–742.
- [32] F. Donnarumma, K.K. Murray, Laser ablation sample transfer for localized LC-MS/MS proteomic analysis of tissue, J. Mass Spectrom. 51 (2016) 261–268.
- [33] F. Donnarumma, F. Cao, K.K. Murray, Laser ablation with vacuum capture for MALDI mass spectrometry of tissue, J. Am. Soc. Mass Spectrom. 27 (2016) 108–116.
- [34] K. Wang, F. Donnarumma, S.W. Herke, P.F. Herke, K.K. Murray, Infrared laser

- ablation sample transfer of tissue DNA for genomic analysis, Anal. Bioanal. Chem. 409 (2017) 4119–4126.
- [35] A. Rohlfing, C. Menzel, L.M. Kukreja, F. Hillenkamp, K. Dreisewerd, Photo-acoustic analysis of matrix-assisted laser desorption/ionization processes with pulsed infrared lasers, J. Phys. Chem. B 107 (2003) 12275–12286.
- [36] J.P. Cummings, J.T. Walsh Jr., Erbium laser ablation: the effect of dynamic optical properties, Appl. Phys. Lett. 62 (1993) 1988–1990.
- [37] M.W. Little, J. Laboy, K.K. Murray, Wavelength dependence of soft infrared laser desorption and ionization, J. Phys. Chem. C 111 (2007) 1412–1416.
- [38] I. Apitz, A. Vogel, Material ejection in nanosecond Er: YAG laser ablation of water, liver, and skin, Appl. Phys. A 81 (2005) 329–338.
- [39] X. Fan, M.W. Little, K.K. Murray, Infrared laser wavelength dependence of particles ablated from glycerol, Appl. Surf. Sci. 255 (2008) 1699–1704.
- [40] F. Cao, F. Donnarumma, K.K. Murray, Particle size measurement from infrared laser ablation of tissue, Analyst 141 (2016) 183–190.
- [41] S. Murakami, M. Kashii, H. Kitano, H. Adachi, K. Takano, H. Matsumura, T. Inoue, Y. Mori, M. Doi, K. Sugamoto, Effect of laser irradiation on enzyme activity, Jpn. J. Appl. Phys. 44 (2005) 8216.
- [42] L. Ren, W. Robertson, R. Reimer, C. Heinze, C. Schneider, D. Eggert, P. Truschow, N.-O. Hansen, P. Kroetz, J. Zou, R.D. Miller, Towards instantaneous cellular level bio diagnosis: laser extraction and imaging of biological entities with conserved integrity and activity, Nanotechnology 26 (2015) 284001.
- [43] K. Franjic, R.J.D. Miller, Vibrationally excited ultrafast thermodynamic phase transitions at the water/air interface, Phys. Chem. Chem. Phys. 12 (2010) 5225—5239
- [44] S.-G. Park, K.K. Murray, Infrared laser ablation sample transfer for MALDI and electrospray, J. Am. Soc. Mass Spectrom. 22 (2011) 1352–1362.
- [45] M.M. Bradford, A rapid and sensitive method for the quantitation of microgram quantities of protein utilizing the principle of protein-dye binding, Anal. Biochem. 72 (1976) 248–254.
- [46] M. Kwiatkowski, M. Wurlitzer, M. Omidi, L. Ren, S. Kruber, R. Nimer, W.D. Robertson, A. Horst, R. Miller, H. Schlüter, Ultrafast extraction of proteins from tissues using desorption by impulsive vibrational excitation, Angew. Chem. Int. Ed. 54 (2015) 285–288.
- [47] J. Zou, C. Wu, W. Robertson, L. Zhigilei, R. Miller, Molecular dynamics investigation of desorption and ion separation following picosecond infrared laser (PIRL) ablation of an ionic aqueous protein solution, J. Chem. Phys. 145 (2016) 204202
- [48] K. Franjic, M.L. Cowan, D. Kraemer, R.D. Miller, Laser selective cutting of biological tissues by impulsive heat deposition through ultrafast vibrational excitations, Opt. Express 17 (2009) 22937–22959.
- [49] I.R. Siqueira, C. Fochesatto, A. de Andrade, M. Santos, M. Hagen, A. Bello-Klein, C.A. Netto, Total antioxidant capacity is impaired in different structures from aged rat brain, Int. J. Dev. Neurosci. 23 (2005) 663–671.
- [50] H.I.M. Homi, J.J. Freitas, R. Curi, I.T. Velasco, B.Á. Junior, Changes in superoxide dismutase and catalase activities of rat brain regions during early global transient ischemia/reperfusion, Neurosci. Lett. 333 (2002) 37–40.
- [51] T. Jayaraman, S. Kannappan, M. Ravichandran, C. Anuradha, Impact of Essentiale L on ethanol-induced changes in rat brain and erythrocytes, Singapore Med. J. 49 (2008) 320—327.
- [52] A.I. Kazi, A. Oommen, Monocrotophos induced oxidative damage associates with severe acetylcholinesterase inhibition in rat brain, Neurotoxicology 33 (2012) 156–161.
- [53] J.J. Fortunato, G. Feier, A.M. Vitali, F.C. Petronilho, F. Dal-Pizzol, J. Quevedo, Malathion-induced oxidative stress in rat brain regions, Neurochem. Res. 31 (2006) 671–678.